Journal of Applied Electrochemistry **31**: 99–104, 2001.

Electrical characteristics of 18650 Li-ion cells at low temperatures

G. NAGASUBRAMANIAN
2521 Lithium Battery R & D, MS: 0613, Sandia National Laboratories, Albuquerque, NM 87185, USA (correspondence: fax: 505/844-6972, e-mail: gnagasu@sandia.gov)

Received 27 March 2000; accepted in revised form 20 July 2000

Key words: energy density, Li-ion cells, power density, Ragone data, three-electrode impedance

Abstract

Low temperature electrical performance characteristics of A&T, Moli, and Panasonic 18650 Li-ion cells are described. Ragone plots of energy and power data of the cells for different temperatures from 25 °C to −40 °C are compared. Although the electrical performance of these cells at and around room temperature is respectable, at temperatures below 0 °C the performance is poor. For example, the delivered power and energy densities of the Panasonic cells at 25 °C are ∼800 W l^{-1} and ∼100 Wh l^{-1}, respectively, and those at −40 °C are <10 W l^{-1} and ∼5 Wh l^{-1}. To identify the source for this poor performance at subambient temperatures, both two- and three-electrode impedance studies were made on these cells. The two-electrode impedance data suggests that the cell ohmic resistance remains nearly constant from 25 to −20 °C but increases modestly at −40 °C while the overall cell impedance increases by an order of magnitude over the same temperature range. The three-electrode impedance data of the A&T cells show that the increase in cell resistance comes mostly from the cathode electrolyte interface and very little either from the anode electrolyte interface or from the ohmic resistance of the cell. This suggests that the poor performance of the cells comes mainly from the high cathode–electrolyte interfacial impedance.

1. Introduction

Approximately nine years ago, Sony Energytec Inc. introduced the first lithium-ion cell into the marketplace. Shortly thereafter, virtually every consumer battery company embarked on development activity aimed at production of this cell. Li-ion cells have a favorable combination of energy and power [1–3] at and around ambient temperatures. Because of this, Li-ion is rapidly taking over the high-performance rechargeable battery market supplanting NiCd and NiMH batteries that cannot meet the energy needs of today's portable electronic products for consumer application. Further, Li-ion is being actively considered for Space and Aerospace applications. For example, NASA is considering Li-ion cells to power Rovers and Landers in Mars Exploration missions. Further, in recent years, the need for power sources is increasing rapidly for a variety of applications including computers, medical, power tools, consumer electronics, and military. The power sources need not only to support many new and additional features in the devices but also need to perform over a wider temperature regime. A thorough and complete understanding of the battery from the point of view of performance, especially at subambient temperatures, is very important for a successful use in these applications. Currently at Sandia National Laboratories, we are evaluating the electrical and electrochemical characteristics of Li-ion cells of different sizes (0.5–40 Ah). These are being studied at ambient and subambient temperatures using a suite of different electrochemical techniques such as impedance and charge/discharge to probe the various electrochemical processes that are occurring in Li-ion cells. The purpose of this study is to identify the component that reduces the cell performance at subambient temperatures. This paper describes our data on the low temperature performance characteristics of A&T, Moli and Panasonic 18650 Li-ion cells.

2. Experimental details

Before welding tabs to the cells for electrical connections, both their weights and physical dimensions were measured. Average values for weights and volume are given in Table 1 along with the cell type, capacity, manufacturer, and the number of cells tested (given in parentheses after the manufacturer's name). Initially, the cells were charged and discharged at room temperature (for at least five cycles) at a very low rate (∼C/20) as 'break-in' cycles. The discharge capacities given in Table 1 represent the average of five cycles per cell and are also averaged over the number of cells tested for that type.

The nominal (rated) cell capacity is slightly higher than the measured discharge capacity. The cells were

Table 1. Physical characteristics and capacities of the lithium-ion cell types

Manufacturer	Rated cell capacity /mAh	Measured discharge capacity /mAh at $C/20$	Weight /g	Cell volume /l
A&T (3)	1400	1370	40.23	0.0168
Moli (5)	1400	1380	41.08	0.0168
Panasonic (3)	1400	1400	39.89	0.0168

charged and discharged at different currents ranging from 20 mA to 5.0 A. An Arbin battery cycler was used (model BT2042, College Station, Texas) up to 1 A and a Macor (Series 4000) battery cycler for currents >1 A. The charge–discharge measurements were also carried out at different temperatures. The cell temperatures during tests were controlled with a Tenney Jr temperature chamber (benchtop model, Union, New Jersey). The cells were charged at a constant current (CC) to 4.1 V followed by clamping of the voltage at 4.1 (CV) and letting the current decay to 10 mA. The cell impedance was measured in the frequency regime from 65 kHz to 0.1 Hz as a function of temperature for two different open circuit voltages (OCVs). For current pulse measurement, a PAR potentiostat/galvanostat (model 273A) was used and the voltage response was captured with a Tektronix oscilloscope (model TDS 754C, Color 4-channel digitizing oscilloscope with Instavu^{TM} Acquisition). The pulse data stored in the oscilloscope were transferred to a computer using a Wavestar program (version 1-0-3) for data processing and plotting. The cells were charged and discharged at different constant currents ranging from 0.02 to 5 A. We performed impedance measurements in a three-electrode configuration (the third electrode being a Li reference electrode) to locate more accurately the source of the problem. The cell configuration was modified to accommodate the Li reference electrode in the mandrel hole that runs along the length of the cell at the centre. Both the bottom and the top of the cell were carefully cut-open in a glove box with a Dremal tool and subsequently tabs were attached to the anode and cathode for electrical contacts. After the cell was opened at both ends it was never exposed to air to prevent degradation of the cell components by reacting with oxygen and water vapour. A Li reference electrode made beforehand was introduced in to the cell through the mandrel hole. The reference electrode assembly consists of a thin platinum wire and a 1 mm diameter glass tube. The platinum wire is fused to one end of the glass tubing. The other end of the platinum wire sticks out the opposite end of the glass tubing for electrical contact. The fused end of the glass tubing was made flat by polishing to form a platinum disc electrode of tiny area and lithium metal was cold-welded to the flat platinum electrode. This completes the reference electrode assembly. The cell with the reference electrode is kept in a plastic beaker to which Sony type electrolyte (ethylene carbonate : propylene carbonate : diethyl carbonate = 1:1:1 v/v containing 1 M $LiPF_6$) was added for impedance studies. The whole assembly was then put in a Kerr Jar for easy handling. The entire operation was performed in a glove box.

3. Results and discussion

3.1. *Charge–discharge characteristics*

The cells were charged and discharged at different constant currents ranging from 0.02 to 5 A.

Typical charge–discharge plot at room temperature for the A&T cell is given in Figure 1. The cell was charged at 0.05 A and discharged at 0.1 A and the capacity remained practically constant (~1370 mAh) even after 20 cycles (not shown). A coulombic efficiency (charge out/charge in) of about 1 was calculated. This, along with a constant cell capacity with cycling, indicates that these Li- ion cells cycle reversibly between the anode and cathode without any apparent parasitic side reactions. Similar results were obtained for the Moli and Panasonic cells. In all three cases, the discharge voltage cutoff was 3.0 V and the charge voltage cut-off was 4.1 V. Similar charge–discharge curves were obtained for different charge and discharge currents. Every discharge curve has over 2000 points, each point corresponding to a voltage. To obtain energy, each voltage is multiplied by the product of discharge current and the time before the voltage jumps to the next level. This procedure is repeated for each voltage, and the results are summed to give the total delivered discharge energy. For discharge power, the voltage is multiplied by the discharge current and the results are summed and averaged over the number of points.

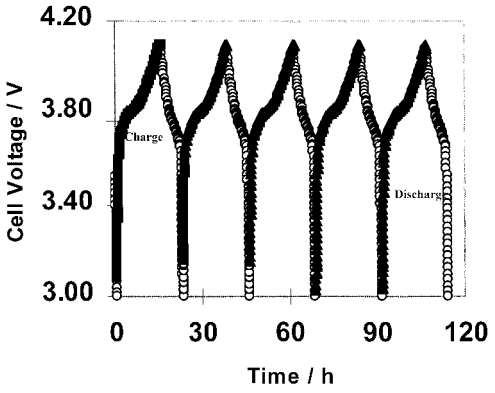

Fig. 1. Charge (□)/Discharge (○) traces for the A&T cell at room temperature. Charge current = 0.05 A and discharge current 0.1 A.

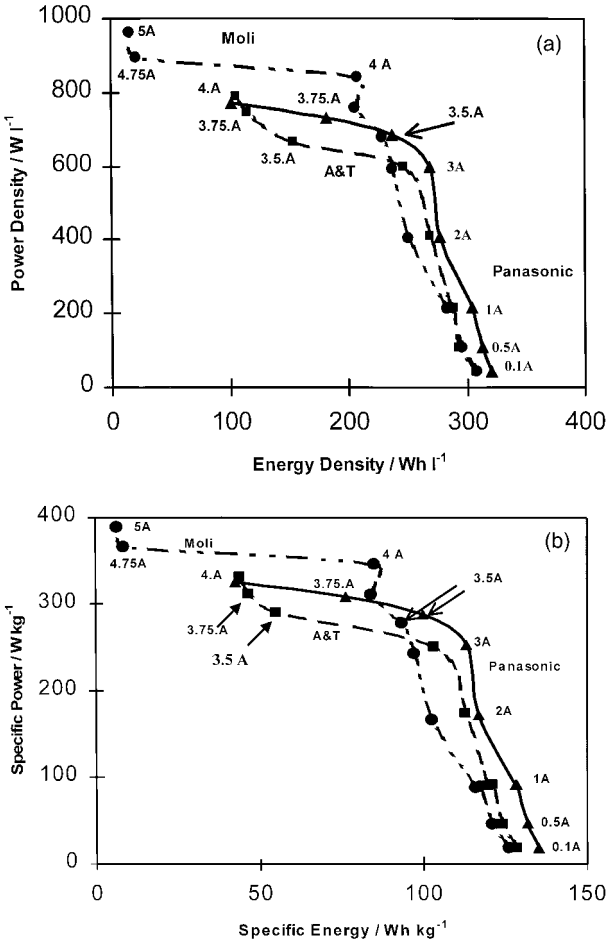

Fig. 2. (a) Power density against energy density for A&T (■), Moli (●) and Panasonic (▲) cells at room temperature. (b) Specific power against specific energy for A&T (■), Moli (●) and Panasonic (▲) cells at room temperature.

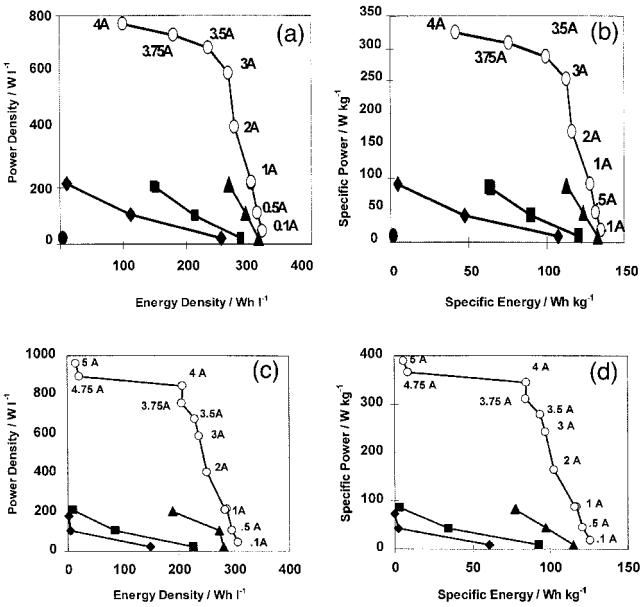

Fig. 3. (a) Power density against energy density for Panasonic cell at different temperatures. (b) Specific power against specific energy for Panasonic cells at different temperatures. Key for (a) and (b): (○) room temp., (▲) 10, (■) −10, (♦) −20 and (●) −40 °C. (c) Power density against energy density for Moli cell at different temperatures. (d) Specific power against specific energy for Moli cells at different temperatures. Key for (c) and (d): (○) room temp., (▲) 10, (■) −10 and (♦) −20 °C.

Ragone plots [2–4] (energy power relationship) at room temperature for the three cells are shown in Figure 2 and the discharge currents are also included in the Figure. In Figure 2(a) the power density (W l^{-1}) against energy density (Wh l^{-1}) is given and in Figure 2(b) the specific power (W kg^{-1}) against specific energy (Wh kg^{-1}) is given. Each data point represents an average of five discharge tests per cell and is also averaged over the number of cells tested for that type (Table 1). The plots indicate that the Li-ion cells have excellent electrical performance at room temperature. For example Moli cells can be discharged at 5 A which corresponds to almost 1000 W l^{-1} at ~15 Wh l^{-1}.

Similar charge/discharge measurements were made at subambient temperatures down to −40 °C and the delivered power and energy are given in Figure 3(a)–(d) along with the room temperature data for comparison. Discharge currents are given in the Figures. No data at subambient temperatures are shown for the A&T cells to avoid over crowding of the plots. In Figure 3(a) and (b) are shown, respectively, for the Panasonic cell the power density against energy density and the specific power against specific energy at different temperatures. Similar plots are shown for the Moli cells in Figure 3(c) and (d). The Ragone plots in Figure 3 indicate that both the delivered energy and delivered power decrease with decreasing temperature and at −40 °C the cells performance is very poor even at 0.1 A discharge.

3.2. *Pulse measurement*

Utilization of portable computing and communication devices and remote monitoring and sensing devices has increased tremendously over the 1990s. The abbreviated time observed in these equipment as well as the transmission of digitized and compressed voice data require high power pulses [5, 6]. In addition, these equipment must be able to operate in a variety of environmental and temperature conditions. To ensure this requirement is satisfied, batteries are subjected to a number of standard tests, including pulse test. In this study we have evaluated the pulse load characteristics of the Li-ion cells under a variety of ambient conditions especially subambient conditions. In Figure 4(a) is given the voltage response as a function of time for a Panasonic cell at −40 °C for a 500 mA constant current 1 s pulse. The voltage response shows an initial sudden drop in voltage followed by slow voltage decay. The initial drop is associated with the ohmic resistance of the cell and the slow voltage decay is due to the interfacial resistance. The voltage drop due to the interfacial charge transfer resistance is more than that

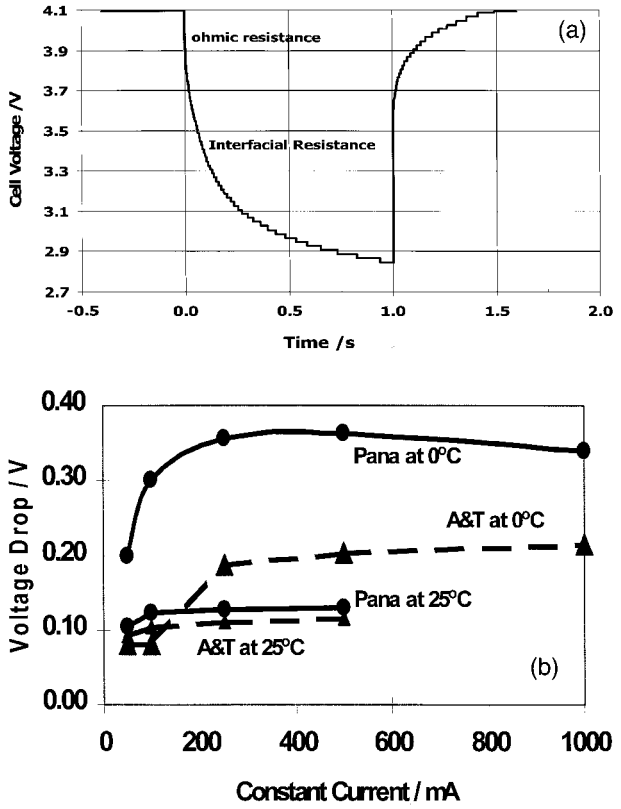

Fig. 4. (a) Cell voltage against time for a 0.5 A constant (1 s) current pulse at −40 °C for a fully charged Panasonic Li-ion cell. (b) Voltage drop for various amplitude current pulses at 25 °C and 0 °C for the A&T and Panasonic cells.

due to the ohmic resistance. If the cell cut-off voltage is 3 V, then the cell has reached the cut-off voltage within 500 ms. In Figure 4(b) are given voltage drop for different current pulses at 25 °C and 0 °C for the A&T and Panasonic cells. The voltage drop plotted in Figure 4(b) includes the voltage drop due to the ohmic resistance and interfacial charge transfer resistance. The voltage drop at 25 °C is lower than that at 10 °C as one would expect and the A&T cell shows a lower voltage drop than the Panasonic cells at the same temperature.

3.3. *Impedance studies*

The charge–discharge and current pulse studies indicate that the electrical performance of the cells at around room temperature is respectable. However, performance degrades rapidly at subambient temperatures. The charge–discharge performance data suggest that the poor performance at subambient temperatures is due to increase in the cell impedance and the pulse data suggests that the poor performance is due mostly to increase in the interfacial resistance. To more accurately pinpoint the source of the problem of whether the impedance increase comes from the ohmic or from the interfacial resistance, we made both two- and three-electrode impedance studies at different temperatures. The two-electrode impedance measurement can discriminate between ohmic and interfacial resistances and the three-electrode (with a reference electrode) can resolve the contributions of the anode and cathode impedances to the total cell impedance.

We made both the two- and three-electrode impedance studies on these cells in the frequency regime 65 kHz to 0.1 Hz with an a.c. signal of 500 μV peak–peak amplitude at different temperatures. The responses of the real and reactive components as a function of frequency for the A&T and Panasonic cells, respectively, are given in the form of a NyQuist plot at different temperatures in Figures 5 and 6. In Figure 5 are given typical NyQuist plots for a fully charged (o.c.v. 4.1 V) A&T cell at different temperatures ranging from 35 to −10 °C. In Figure 6 similar plots are given for a fully charged (o.c.v. 4.1 V) Panasonic cells. The NyQuist plots show an inductive tail in the frequency regime 65–2.7 kHz followed by two humps at lower frequencies. The hump closer to the inductive tail is smaller than the other. The inductive tail has been observed by others for Li–MoS_2 cells [7] and in that case has been attributed to the jellyroll and/or porous electrode designs. The inductive tail in the case of these cells could also be due to a similar design feature. The ohmic cell resistance (high frequency x-axis intercept) includes electrolyte resistance and other series resistances such as electrode

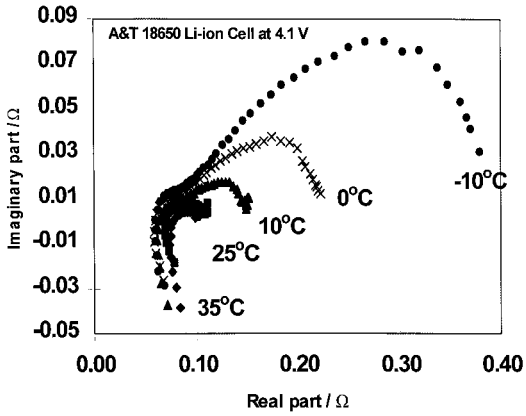

Fig. 5. Typical NyQuist plots for a fully charged (o.c.v. 4.1 V) A&T cell at different temperatures.

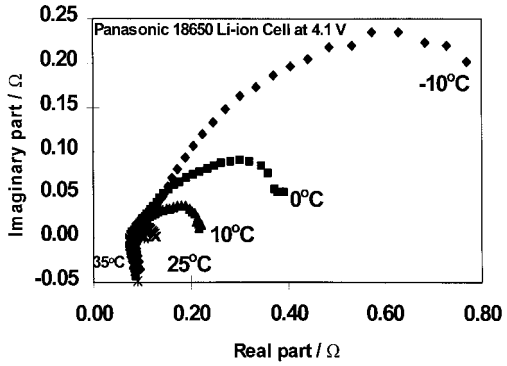

Fig. 6. Typical NyQuist plots for a fully charged (o.c.v. 4.1 V) Panasonic cell at different temperatures.

bulk resistance, separator resistance and PTC resistance. This resistance, is small (~0.08 Ω). However, the overall cell impedance including ohmic resistance, cathode electrolyte R_{ct}, (charge transfer resistance + solid electrolyte interphase (SEI) resistance), and anode electrolyte R_{ct} is higher (several ohms) at lower temperatures. For example, at −10 °C the ohmic resistance is only around 80 mΩ while the overall cell impedance is about 400 mΩ. The high frequency intercept, which corresponds to the ohmic resistance of the cell, is given in Figure 7 as a function of temperature for the fully charged and fully discharged A&T and Panasonic cells. The ohmic resistance is very nearly the same for the charged and discharged cells. The ohmic resistance of the cell remains nearly constant from 35 to −20 °C. However, at −40 °C there is a modest increase in ohmic resistance. This observation clearly indicates that the progressive decline in cell electrical performance with temperature going down is: (i) not due to the ohmic resistance and (ii) probably coming from the cathode and anode interfacial resistances. However, the two-electrode study does not tell us which one of the interfaces (cathode, anode or both) are responsible for the performance decline. The three-electrode impedance data for the A&T cell at 25 °C are shown in Figure 8 along with the two-electrode impedance data of the opened cell. The plots clearly show that the cathode electrolyte interfacial impedance is significantly higher than either the anode electrolyte interface or the ohmic resistance. Similar impedance behavior was observed for the Moli and Panasonic cells also. We also checked if the placement of the reference electrode (within or outside of the cell) makes a difference in the impedance data. We did not note any change in the cathode and/or anode impedance measured by placing the reference electrode in two different positions which suggests that the placement of the reference electrode did not alter the cell impedance.

Cell impedance data published earlier by Ozawa [8] is in contrast to our data. These data were obtained from two-electrode impedance measurements. He has assigned the large 2nd loop in the NyQuist plot to the anode and the smaller (at higher frequencies) to the cathode.

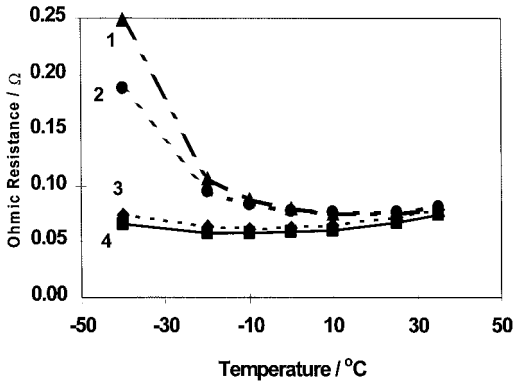

Fig. 7. Plots of ohmic resistance against temperature for the fully charged (2 and 4) and fully discharged (1 and 3) A&T and Panasonic cells, respectively.

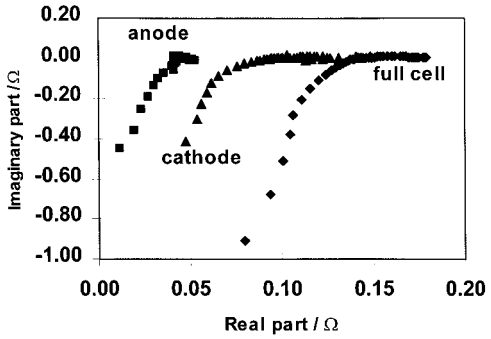

Fig. 8. NyQuist impedance plots for the A&T full cell (♦) at 4.1 V (obtained from two-electrode impedance data) and its cathode (▲), anode (■) electrodes (obtained from three-electrode impedance data) measured at room temperature.

4. Conclusions

We evaluated the electrical performance characteristics of A&T, Moli and Panasonic 18650 Li-ion cells at different temperatures. Although the electrical performance of these cells at and around room temperature is respectable, at temperatures below 0 °C the performance is poor. For example, the delivered power and energy densities of the Panasonic cells at 25 °C are ~800 W l^{-1} and ~100 Wh l^{-1}, respectively. However, at −40 °C the delivered power and energy are <10 W l^{-1} and ~5 Wh l^{-1}. The two- and three- electrode impedance studies on the cells indicate that: (a) the ohmic resistance of the cell is nearly constant from 35 to −20 °C but increases modestly at −40 °C, (b) the overall cell impedance increases by more than 10 times going from 35 to −40 °C, and (c) the increase in cell impedance at subambient temperatures is mostly due to the increase in the interfacial resistance (charge transfer + SEI resistance) of the cathode–electrolyte interface which is responsible for the poor cell performance.

Acknowledgement

Sandia National Laboratories is a multiprogram laboratory operated by Sandia Corporation, a Lockheed Martin Company, for the United States Department of Energy under contract DE-AC04-94AL85000. I am grateful to D.R. Bradley for performing the electrochemical measurements.

References

1. G. Nagasubramanian and R.J. Jungst, *J. Power Sources* **72** (1998) 189–93.
2. B.A. Johnson and R.E. White, *J. Power Sources* **70** (1998) 48.

3. *Solid State Ionics* **69** (1994), several papers in this issue.
4. D. Ragone, *in* Proc. Soc. Automotive Engineers Conference, Detroit, MI, May (1968).
5. E. Peter Roth and G. Nagasubramanian, *in* 38th Power Sources Conference, Cherry Hill, NJ, 8–11 June (1998).
6. A. Anani, F. Eschbach, J. Howard, F. Malaspina and V. Meadows, *Electrochim. Acta* **40** (1995) 2211.
7. F.C. Laman, M.W. Matsen and J.A.R. Stiles, *J. Electrochem. Soc.* **133** (1986) 2441.
8. K. Ozawa, *Solid State Ionics* **69** (1994) 212.